Available online at www.sciencedirect.com
ScienceDirect
International Journal of Mass Spectrometry 268 (2007) 207–216
International Journal of Mass Spectrometry
www.elsevier.com/locate/ijms

Mass spectrometric characterization of conformational preludes to β_2-microglobulin aggregation

Thomas J.D. Jørgensen [a,*], Lei Cheng [a], Niels H.H. Heegaard [b]

[a] *Department of Biochemistry and Molecular Biology, University of Southern Denmark, Campusvej 55, 5230 Odense M, Denmark*
[b] *Department of Autoimmunology, Statens Serum Institut, Copenhagen, Denmark*

Received 23 April 2007; received in revised form 21 July 2007; accepted 31 July 2007
Available online 6 August 2007

Abstract

Characterization of protein folding and unfolding is an important issue for basic biological science, for understanding the devastating amyloid diseases, and for the manufacture and use of biological therapeutics. Unlike nuclear magnetic resonance spectroscopy, the use of mass spectrometry to monitor amide hydrogen ($^1H/^2H$) exchange kinetics (HX-MS) allows characterization of structural dynamics even when only limited amounts of protein is available. As an adjunct technique, requiring even less material and very well suited for serial monitoring of folding phenomena in a single solution under native conditions capillary electrophoresis may also be very informative. These approaches are here used to examine the small (99 amino acid residues) protein β_2-microglobulin (β_2m) which is prone to amyloidogenic unfolding especially after cleavage at its lysine-58 residue. The propensity for unfolding of native, non-cleaved β_2m and lysine-58 cleaved β_2m variants as well as the effect of acetonitrile on the conformational equilibria could be addressed by these approaches. At physiological conditions, intact β_2m and the lysine-58 cleaved variants undergo a transient unfolding that exhibit an EX1 type hydrogen exchange behaviour. We have measured the unfolding rate constants for the cleaved variant where Lys-58 is removed (ΔK58-β_2m) and the cleaved variant where this residue is preserved (cK58-β_2m) at various temperatures. Below 37 °C, the variant devoid of Lys-58 (ΔK58-β_2m) has a higher unfolding rate than cK58-β_2m and this correlates with the observation that ΔK58-β_2m has a higher propensity to aggregate. The results of our studies provide valuable insight into the early conformational perturbations involved in rendering this protein insoluble and amyloidogenic. The approaches used in this study should be useful also for the characterization of other conformationally unstable proteins.

Keywords: Amyloid; Hydrogen exchange; Conformation; EX1; β_2-Microglobulin

1. Introduction

Protein aggregation and misfolding have profound implications for human disease and for the use and safety of protein-based biological drugs. Protein conformation is also of interest for understanding protein function in the normal organism. In the amyloidoses, a specific subgroup of protein conformational diseases, the aggregated proteins or peptides attain insoluble cross β-sheet structures called amyloid. Such structures are formed, e.g., in central nervous system-amyloidoses by the amyloid β-peptides in Alzheimer's disease and by synuclein in Parkinson's disease. In the group of systemic amyloidoses the malfolding culprits are, e.g., acute-phase protein and immunoglobulin fragments [1]. In dialysis-related amyloidosis (DRA), the aggregating protein is β_2-microglobulin (β_2m). β_2m-Amyloidosis is observed in patients with kidney disease and long-term hemodialysis treatment [2,3]. It involves the deposition of this normally well-soluble small serum protein as amyloid fibrils in osteoarticular structures leading to complications including carpal tunnel syndrome, bone cysts, and arthropathies [4]. Native β_2m is rich in β-strands [5] and is very soluble in striking contrast to the extreme insolubility of β_2m aggregated as amyloid. Most of the aggregated β_2m appears to be intact with respect to primary structure [6] although a subfraction of cleaved molecules may be extracted from the fibril material [7–10] and although a significant number of dialysis patients have cleaved β_2m (ΔK58-β_2m) where

Abbreviations: β_2m, β_2-microglobulin; cK58-β_2m, β_2m cleaved after K58; ΔK58-β_2m, β_2m cleaved after and devoid of its K58-residue; CE, capillary electrophoresis; DRA, dialysis-related amyloidosis; wt, wild-type; HX-MS, amide hydrogen ($^1H/^2H$) monitored by mass spectrometry

* Corresponding author. Tel.: +45 6550 2414; fax: +45 6550 2467.
E-mail address: tjdj@bmb.sdu.dk (T.J.D. Jørgensen).

1387-3806/$ – see front matter © 2007 Elsevier B.V. All rights reserved.
doi:10.1016/j.ijms.2007.07.020

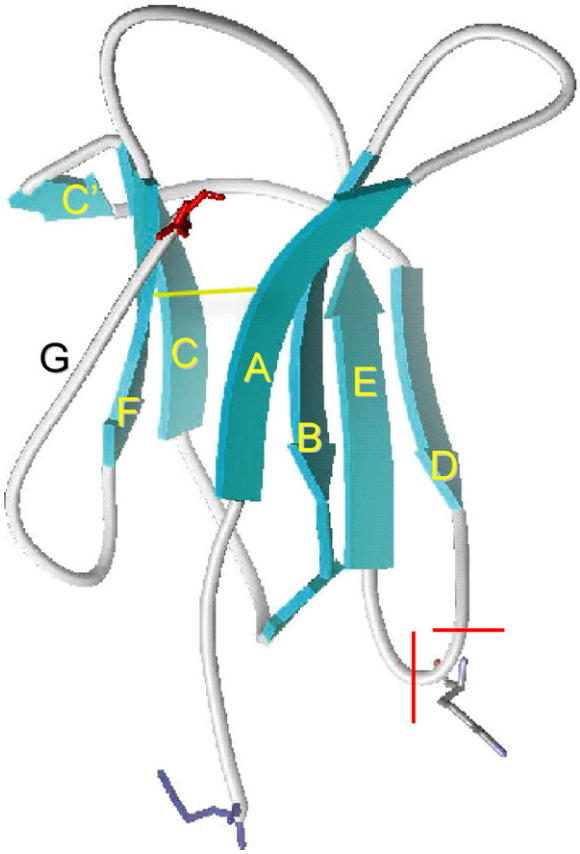

Fig. 1. Crystal structure of intact β_2m. The ribbon diagram was drawn with WebLab ViewerPro (PDB number 1LDS) [50]. The red lines indicate the cleavages of the polypeptide chain for the cleaved variant of β_2m where Lys58 is removed from the loop-connecting strands D and E (ΔK58-β_2m).

the K58-residue has been removed [11] present in the circulation. The loop connecting strands D and E where K58 resides is a favourite site for limited proteolysis of β_2m, especially in conditions where an activated complement system is encountered [12] (Fig. 1). It is unknown how native, wild-type (wt) β_2m is transformed into β_2m-amyloid, but it is assumed that some, possibly small, conformational change is responsible for early events on the pathway to amyloid aggregation [13]. We and others have devised analytical methods, particularly capillary electrophoresis (CE) for assessing β_2m conformational variants under native conditions [13,14]. It was found that a well-defined alternative conformation is significantly populated by β_2m-variants cleaved at lysine-58, i.e., ΔK58 and cK58-β_2m, [15]. It was also found by CE that the presence of organic solvent tends to induce an increased conformational heterogeneity of wt-β_2m to a degree that it resembles the conformer profile of ΔK58-β_2m [16]. Amide hydrogen (^{1}H/^{2}H) exchange monitored by mass spectrometry subsequently revealed that in fact both wt and cleaved β_2m undergo transient unfolding, and that the cleaved molecule (ΔK58-β_2m) is considerably more prone to unfold than intact β_2m molecules. Thus, unfolding rates at physiological temperatures are almost 10 times higher for cleaved than for intact wt-β_2m [17]. The previously published results further showed an increased aggregation tendency of the cleaved ΔK58-β_2m and indicated a pronounced influence of temperature on aggregation and unfolding rates for both wild-type and cleaved β_2m [18]. Regions and residues involved in refolding from partially denatured states of β_2m were previously partially characterized by NMR spectroscopy [19–28]. The characterization of unfolding from the native state has been less accessible by NMR, since conformational states other than the fully folded in wild-type β_2m are sparsely populated under physiological conditions and are in equilibrium with the native conformation, and since rather high protein concentrations – where the cleaved variants aggregate and precipitate – are required for these measurements [18]. It is therefore not readily possible to investigate the quantitative dynamics of β_2m and cleaved β_2m unfolding using ensemble spectroscopic techniques such as NMR spectroscopy.

We here report the utility of capillary electrophoresis and mass spectrometry-monitored isotopic exchange reactions to assess the influence of temperature and organic solvent on the conformational equilibria of wt and the two cleaved variants. The increased aggregability of K58-cleaved β_2m appears to be directly dependent on the increased unfolding kinetics of the cleaved variants which could be readily quantitated by the techniques used in this study. The pronounced influence of temperature on the unfolding kinetics was also illustrated by the results and it could be shown that an almost complete acetonitrile-induced unfolding required 25 °C while at 0 °C the extent of unfolding was indistinguishable from the unfolding in the absence of organic solvent. Finally, the experiments allowed quantitative estimate of the activation energy for unfolding of cleaved β_2m (cK58-β_2m).

2. Materials and methods

2.1. Chemicals and biological materials

Human β_2m and β_2m cleaved at lysine-58, and cleaved β_2m with lysine-58 deleted (cf. Fig. 1) were purified and produced from human nephropathy patient urine as previously detailed [29]. Specific reagents for the hydrogen (^{1}H/^{2}H) exchange experiments were deuterium oxide (D_2O, 99.9% D) from Cambridge Isotope Laboratories (Andover, MA, USA) and otherwise as specified in Ref. [17]. Isotopic exchange of β_2m took place in deuterated phosphate-buffered saline (10 mM phosphate, pH 7.4 containing 2.7 mM potassium chloride and 137 mM sodium chloride). The protiated buffer was deuterated by redissolving it in D_2O after lyophilization. This process was repeated twice.

2.2. Capillary electrophoresis

CE analyses were performed in Beckman P/ACE 2050 or 5010 instruments with sample temperature control. Detection took place at 200 nm, capillary cooling at 15 or 20 °C, and a 57 cm long (50 cm to the detector), 50 μm diameter uncoated fused silica capillary was used unless otherwise specified. Injection volumes and separation modes are specified in the figure texts. The marker molecule was a synthetic *N*-acetylated tetrapeptide of the sequence Ac-PSKD-OH. Samples (20–30 μL) were protected against evaporation by a 20 μL overlayed volume of light mineral oil [14].

2.3. Amide hydrogen ($^1H/^2H$) exchange and the set-up for rapid desalting

Incubation in deuterated buffer was performed in an Eppendorf Thermomixer at the temperatures indicated. Isotopic exchange was initiated by a 50-fold dilution of a β_2m solution (1–2 mg/mL) into deuterated PBS (e.g., 10 μL β_2m solution + 490 μL PBS buffer). Aliquots were secured at defined times and amide hydrogen exchange was quenched by lowering the pH to ∼2.2 by adding 2.5% trifluoroacetic acid to a final concentration of 0.1% and flash freezing the solution in liquid N_2. The aliquots were stored in liquid N_2 until MS analysis.

The equipment for rapid desalting was previously described [17]. It consists of two HPLC pumps (Applied Biosystems Model 140B), an injection valve (Rheodyne Model 7725i), and a computer controlled 10-port two-position HPLC valve (Valco Model C2-1000A) equipped with a self-packed reversed phase C_{18} microcolumn [30]. All components that were in contact with the samples were immersed in a ice-water slurry at 0 °C to minimize the deuterium loss caused by back-exchange with the protiated HPLC solvents. The quenched samples that were secured from the isotopic exchange experiments were thawed individually before injection. Injection took place by an ice-cold HPLC syringe into a stainless steel loop mounted on the injection valve. The total time for desalting and elution was 2 min. Back-exchange control experiments were carried out to quantify the inevitable deuterium loss that occurs during desalting and elution at quench conditions where the exchange kinetics of main-chain amide hydrogens is slow. Intact β_2m contains a total of 93 main-chain amide hydrogens. Aliquots of fully deuterated intact β_2m were subjected to rapid desalting and MS-analysis. A maximum content of 84 ± 3 deuterons atoms was observed, i.e., approximately 10 deuterons are back-exchanged with protons during quench conditions. No adjustment for this artifactual deuterium loss has been made, as our main focus is the correlated exchange kinetics which is not affected by this loss.

2.4. Mass spectrometry and data analysis

Positive ion ESI mass spectra were acquired on a Micromass (Manchester, UK) quadrupole time-of-flight mass spectrometer (Q-TOF 1) equipped with an electrospray ion source. Ion source settings were: capillary voltage 3.0–3.5 kV, cone voltage 55 V, ion source block temperature 80 °C, nebulizer gas flow 20 L/h (25 °C), desolvation gas flow 400 L/h (200 °C). Nitrogen was used for nebulization and desolvation. The instrument was calibrated using apomyoglobin. Mass spectra were acquired for the mass range m/z 500–2000.

Mass spectra were processed using Masslynx software (v. 3.5) and deconvolution was carried out with the maximum entropy algorithm (MaxEnt 1) included in this software. Unfolding rate constants were obtained by fitting a bi-exponential equation to the abundance ratios, $[I_{low}/(I_{low} + I_{high})]$, that were determined from mass spectrometric peak areas [17]. The fitting process was performed with the constraint $k_u = k_{u,Ox}$. The unfolding rate constants, k_u, and corresponding half-lives, $t_{1/2}$, for the cleaved variants of β_2m (i.e., ΔK58-β_2m and cK58-β_2m) were determined from exchange experiments where the proteins were incubated together in deuterated buffer. The experimental conditions (exchange time, temperature, pH, etc.) are thus completely identical for the two proteins. This means that the experimental uncertainty for the relative difference in their unfolding rates at a given temperature is small compared to the experimental uncertainty of the measurement of absolute unfolding rate constants. In the present experiments, a coefficient of variation (CV) of 12% was obtained for a triplicate determination of k_u for wt-β_2m. The activation energy, E_a, for unfolding was determined from an Arrhenius plot, where the slope of $\ln k$ versus $1/T$ corresponds to $-E_a/R$. Note that E_a and the activation enthalpy for unfolding, ΔH°, only differ by the term RT (∼2.5 kJ/mol) [31]. This difference is within our experimental uncertainty.

3. Results and discussion

Previous studies of intact and lysine-58 cleaved β_2m (ΔK58-β_2m) (Fig. 1) by NMR spectroscopy and circular dichroism yielded some information about the content of structural elements and overall conformation of the two species. NMR showed no major differences with respect to overall conformation but revealed signs of increased conformational heterogeneity in the cleaved forms of β_2m [18]. Circular dichroism studies showed some differences between intact and cleaved species of β_2m [15] compatible with partial loss of β-structures and/or increased conformational heterogeneity. However, no detailed and quantitative information on the conformational structures involved in these differences could be extracted from these experiments. When analyzed by capillary electrophoresis under nondenaturing conditions (Fig. 2), a mixture of the two molecules is well separated, first of all because ΔK58-β_2m, which is lacking a lysine residue, is more negatively charged than intact β_2m. In addition, the individual molecules both fractionate

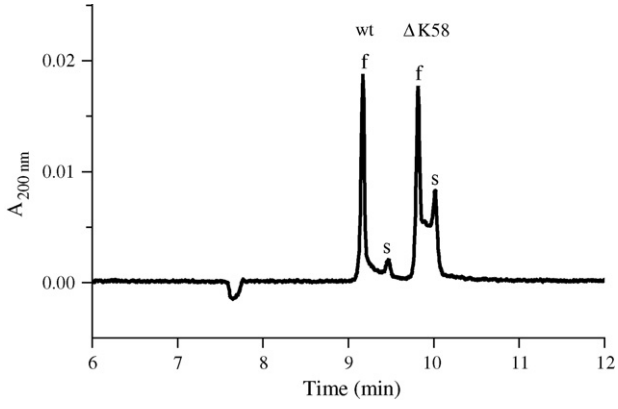

Fig. 2. Increased heterogeneity of the separation profile of cleaved β_2m in capillary electrophoresis (CE) analysis. An approximately equimolar (15 μM) mixture of intact β_2m and the cleaved form ΔK58-β_2m was analyzed in solution using 0.1 M phosphate, pH 7.4 as electrophoresis buffer using a constant current of 80 μA for the electrophoresis. The capillary was thermostatted at 20 °C. The f- and s-peaks are indicated and it is readily apparent that the s-peak and the intermediate plateau are significantly increased in cleaved β_2m (ΔK).

into a major peak (the f-peaks) and a slower, minor component (the s-peaks). The s-peak represents less than 10% of the total peak area of intact β_2m but much more in ΔK58-β_2m which, in addition, displays a clearly elevated intermediary plateau joining the f- and s-peaks. Since no contaminating molecules can be detected by other techniques we conclude that these observations are due to the existence of more than one conformation in the β_2m solutions with the intermediary plateau representing molecules that attain more than one conformation during the time it takes for the analytes to arrive at the detector window [32]. We found that the plateau height and s-peak area were highly dependent on the sample temperature and also that combinations of physiological temperature and high protein concentrations inevitably lead to a time-dependent formation of oligomeric species, and aggregation and precipitation of cleaved in contrast to intact β_2m [17,18].

CE analyses also showed that treatment with organics such as acetonitrile, ethanol, and trifluoroethanol induces an increased conformational heterogeneity of intact β_2m [16]. This is illustrated in Fig. 3 where the same preparation of intact β_2m in the absence or presence of 50% acetonitrile in the sample solution is analyzed. It is readily apparent that while the total peak area is approximately constant, the formation of the s-peak is greatly enhanced in organic solvent. The experiments of Figs. 2 and 3 were performed under different separation conditions explaining the differences in peak appearance times.

Increasing conformational instability as a consequence of cleavage at K58 and as a consequence of exposure to organic solvent was clearly evidenced by the CE analyses. However, a more detailed understanding of the extent of the unfolding required the application of other analytical methods. For this purpose mass spectrometric monitoring of amide hydrogen (^{1}H/^{2}H) exchange (HX-MS) was applied. This approach has the advantage that the number of solvent-exposed non-protected back-bone amide hydrogens are directly measured from mass changes over time [33]. In a natively folded protein, amide hydrogens that participate in stable hydrogen-bonded structures are protected against isotopic exchange with the solvent. For exchange to occur, the catalyst ion (i.e., deuteroxide: OD^-) must gain direct access to the amide hydrogen to facilitate its abstraction. This yields an amidate anion, which in turn rapidly reacts with D_2O, whereby the exchange reaction is completed [34]. In the deuterium exchange-in experiment, isotopic exchange is initiated by incubating the protein in deuterated buffer. The protein mass increases gradually with time as transient unfolding processes break protecting hydrogen bonds and allow isotopic exchange to proceed. Unstructured or very dynamical regions undergo rapid exchange on a sub-second time scale, while more stable hydrogen-bonded regions may require several days to exchange.

Since it appeared from the CE experiments that an increased population of an alternative conformation (the s-peak, Fig. 3) could be induced in intact β_2m by treatment with organic solvent, we used HX-MS to probe the effect of organic solvent and temperature on the opening of the intact molecule. Fig. 4(a) shows the mass spectrometric peak corresponding to the +10 charge state, $[M+10]^{10+}$, of nondeuterated β_2m wt. Note the

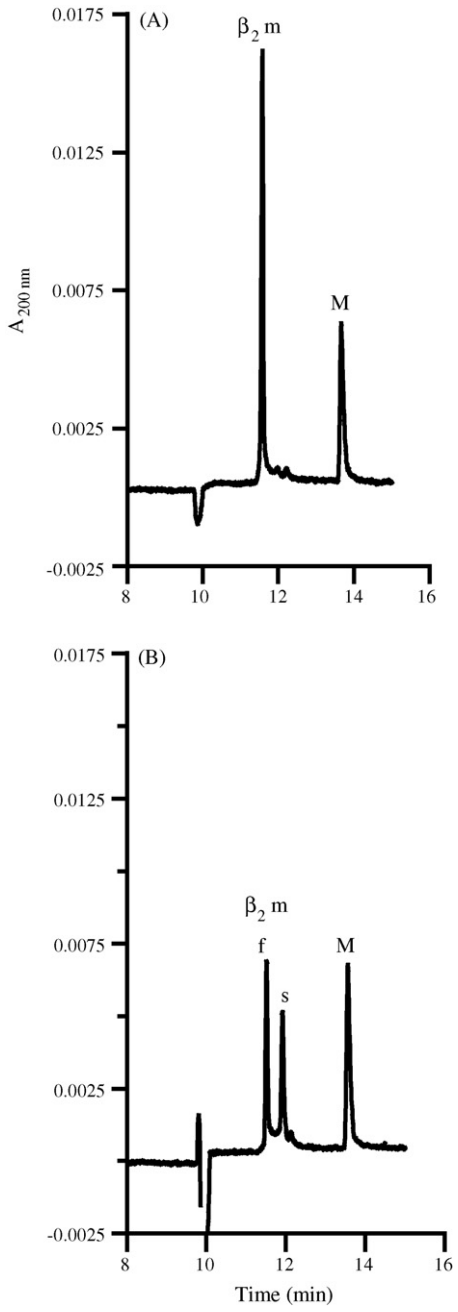

Fig. 3. Electrophoretic separation profile of wt-β_2m is greatly influenced by organic solvent. An aliquot of β_2m (0.7 mg/mL) together with a marker peptide (M) at 0.1 mg/mL in dilute phosphate-buffered saline, pH 7.4 was mixed 1:1 with either water (A) or acetonitrile (B). The temperature of the mixtures at injection was 25 °C. The CE analyses were carried out as described in Fig. 2 using a constant voltage of 16 kV and capillary thermostatting at 15 °C.

presence of a minor +16 Da peak (labeled Ox) that represents oxidized β_2m. The C-terminal amino acid of β_2m is a methionine which is prone to oxidation [35,36]. A short incubation period (25 s) of β_2m wt in deuterated buffer at 25 °C causes incorporation of ~51 deuterium atoms (Fig. 4(b)). When wt-β_2m is preincubated in 1:1 PBS/CH_3CN at 25 °C prior to isotopic exchange at 25 °C, however, ~84 deuterium atoms are incorporated (Fig. 4(c)). This deuterium level corresponds to fully deuterated β_2m (cf. Section 2). Thus, the addition of

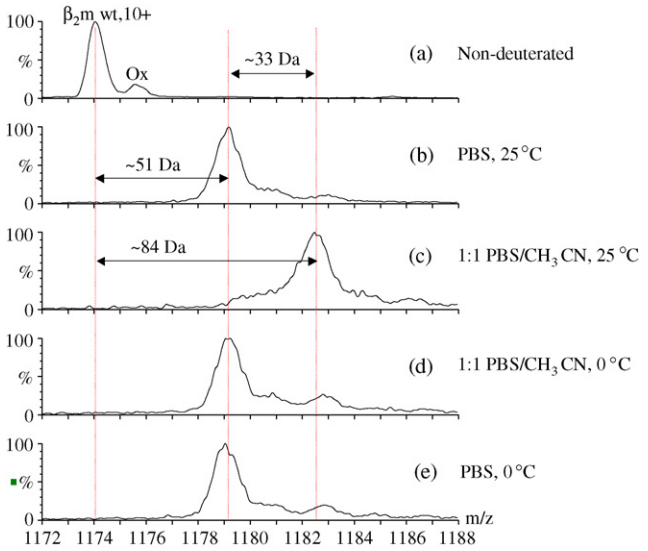

Fig. 4. The effect of organic solvent and temperature on the conformational equilibrium of wt-β_2m. Amide $^1H/^2H$ exchange on wt-β_2m after 60 min preincubation in PBS buffer in the presence (c and d) or absence (b and e) of 50% acetonitrile at (b and c) 25 °C and (d and e) 0 °C. Shown are ESI mass spectra of $[wt\text{-}\beta_2m + 10H]^{10+}$ obtained after deuteration for 25 s at 0 °C. Spectrum (a) shows the peaks corresponding to the nondeuterated protein and the oxidized (+16 Da) species. The average mass differences are indicated by dotted lines and illustrate that in the presence of 50% acetonitrile at 25 °C, wt-β_2m predominantly populates the unfolded state.

acetonitrile induces a dramatic shift in conformer equilibrium toward unfolded states at 25 °C. In contrast, preincubation under the same conditions but at a lower temperature (0 °C) does not cause unfolding of wt-β_2m as only ∼51 deuterium atoms are incorporated (Fig. 4(d)). The native conformation appears to be preserved at these conditions since the same deuterium level is observed in the absence of acetonitrile. Thus, folded intact β_2m, even in 50% acetonitrile at 0 °C, contains ∼33 protected amide hydrogens. When the temperature is increased to 25 °C in the presence of acetonitrile, the protein structure is thermally destabilized and the unfolded state is predominantly populated. The organic solvent conditions at 25 °C render all available amide hydrogens accessible to the solvent suggesting that no protecting hydrogen bonds remain under these conditions. In apparent contrast, the results obtained by CE show that the folded state (f-peak) is more populated than the unfolded state (s-peak) at these conditions (Fig. 3B). This apparent discrepancy between HX-MS and CE results is, however, primarily due to differences in the time-scale between these two techniques. In the HX-MS experiments at 25 °C, the unfolded proteins in 50% acetonitrile will begin to refold when they are diluted into deuterated buffer. The refolding of β_2-microglobulin is, however, a slow process (as evidenced by the EX1 kinetics, see below) and all back-bone amide groups are therefore completely deuterated before the protein has refolded. In the CE experiments, the protein also begins refolding upon injection, but it takes approximately 10 min for the protein to reach the detector. Within this period, the majority of the protein molecules has refolded and this results in the appearance of two peaks (i.e., the f- and s-peaks in Fig. 3B).

3.1. Unfolding kinetics for cleaved β_2m variants

Deuteration of a natively folded protein typically yields a single mass spectrometric peak that gradually increases in mass with a nearly constant peak width. This type of exchange behaviour is termed EX2 [33,37,38], and it reflects that the life-time of the exchange-competent open state of the protein is short relative to the time-scale for the chemical exchange reaction. For β_2m, however, we encountered a different type of exchange behaviour as short deuteration periods yielded a single peak, whereas prolonged deuteration lead to the appearance of a bimodal peak pattern[1] [17]. Such a pattern is a mass spectrometric signature of the more rare EX1 type of exchange [39,40]. In this case, the life-time of the transiently unfolded state is sufficiently long to allow simultaneous exchange of the group of solvent-exposed amide hydrogens within a single opening event. This means that the rate of the transient unfolding reaction can be obtained directly from the rate of the appearance of the higher mass peak in the bimodal peak pattern. This peak represents the population of molecules that have undergone unfolding, while the lower mass peak represents molecules that have not yet been unfolded in the deuterated buffer. Fig. 5 exemplifies these peaks as well as the populations of deuterated species for ΔK58-β_2m and β_2m wt. Fig. 6(a) illustrates schematically the correlated exchange mechanism involving all amide hydrogens in an transiently fully unfolded α-helix. Also shown is the appearance of a bimodal peak pattern when this type of unfolding is analyzed by HX-MS. Fig. 6(b) shows a non-correlated exchange mechanism in an α-helix. The mass difference of a bimodal peak gives direct information about the number of amide hydrogens that becomes exposed to the solvent during the unfolding process. It should be noted, however, that this mass difference does not remain constant throughout the exchange experiment. To illustrate this, consider the two aforementioned molecular populations and assume that the unfolding is global and causes complete deuteration of the protein. For this protein, the lower mass population contain a number of nondeuterated protected amides. If global unfolding was the only structural transition that caused exchange at these protected sites then the lower mass peak would remain at a constant *m/z* value during the experiment. But the protein structure is dynamic and local transient structural fluctuations break protecting hydrogen bonds and causes a gradual non-correlated exchange of these protected amides. Thus, the lower mass population slowly increases in mass as a result of the local conformational flexibility of the folded state, while the higher mass population is fully deuterated and thus remains constant. Consequently, the mass difference decreases between the bimodal peaks at prolonged deuteration. This phenomenon can be utilized by HX-MS to separately investigate the occurrence of large-scale motions of the polypeptide chain in global unfolding processes (i.e., correlated exchange) and the local

[1] A single peak is observed for the nonoxidized protein at short deuteration periods. Note, however, that preparations of β_2m usually contains oxidized β_2m (+16 Da), which must be taken into account in the data analysis. β_2m is purified from human urine and the amount of oxidized protein varies from batch to batch.

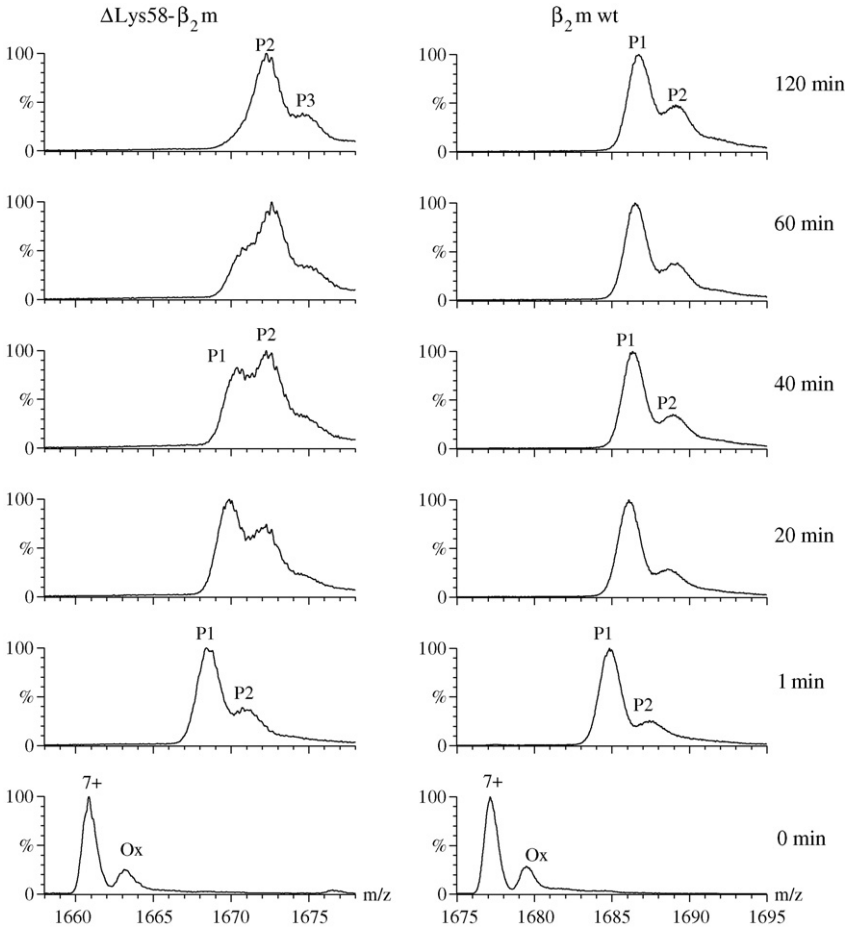

Fig. 5. Monitoring the transient global unfolding of β_2m wt and ΔK58-β_2m at 30 °C by amide $^1H/^2H$ exchange and mass spectrometry. Shown are electrospray ionization (ESI) mass spectra of ΔK58-β_2m (left panel) and β_2m wt (right panel) obtained after various deuteration periods (given in minutes in the figure). The region of the spectra with the $[M+7H]^{7+}$ charge state is displayed; Ox, Met99-oxidized species. The spectra obtained at $t = 0$ min (i.e., lowest traces) show the nondeuterated proteins. P1 indicates the lower mass population which represents partially deuterated nonoxidized molecules that have not undergone global unfolding in the deuterated buffer. P2 indicates the higher mass population which is comprised of nonoxidized molecules that have undergone global unfolding in deuterated buffer. P2 also indicates the oxidized molecules that have not yet visited the globally unfolded state. Note that the two populations in peak P2 are close in mass and cannot be resolved in this experiment. However, the kinetic equation to determine unfolding rate constants take both populations into account [17]. P3 indicates the highest mass population which represents oxidized molecules that have undergone global unfolding in deuterated buffer. It is clearly seen that the intensity of the P2 peak for ΔK58-β_2m increases at a faster rate than that of β_2m wt. This reflects directly the accelerated unfolding of ΔK58-β_2m.

motions of the chain in natively folded state (i.e., non-correlated exchange). This is possible as these two distinct structural transitions yield two populations with different masses. Note that such a distinction between exchange mechanisms at a fixed pH value is not possible with other spectroscopic techniques (e.g., NMR).

Very recently, we have used HX-MS to probe how the conformational flexibility of the folded state is affected by cleavage of the polypeptide chain at Lys58 which resides in a loop connecting strand E and D (Fig. 1) [18]. In this study we determined the non-correlated exchange kinetics for ΔK58-β_2m, cK58-β_2m and β_2m wt to investigate whether they display similar conformations in their folded state. It was also of interest to ascertain whether the local transient structural fluctuations of the most protected amides were different in these three proteins. It should be noted that prior to this investigation, we reported that the unfolding kinetics of ΔK58-β_2m is almost an order of magnitude greater than that of β_2m wt [17]. Thus, cleavage of the polypeptide chain and removal of Lys58 destabilizes the folded state as evidenced by the accelerated rate for transient global unfolding. In contrast, we observed only a very small difference in the magnitude of local fluctuations of the protected amides between, on the one side, the cleaved variants of β_2m and on the other side the wild-type [18]. This result shows that cleavage at Lys58 has only minor effects on protecting hydrogen bonds in the protein. In other words, the loop cleavage predominantly increases the motility of the polypeptide chain locally around the cleavage site but leaves the rest of the protein structure unperturbed. A somewhat similar effect was observed by Maity et al. [41] when a replacement of a lysine residue with glycine in cytochrome *c* caused a local increase in the flexibility of the polypeptide chain around the Gly residue, whereas most residues located elsewhere in the protein were not affected. The global stability of the protein was, however, decreased by the substitution, i.e., the folding–unfolding equilibrium was shifted toward the unfolded state.

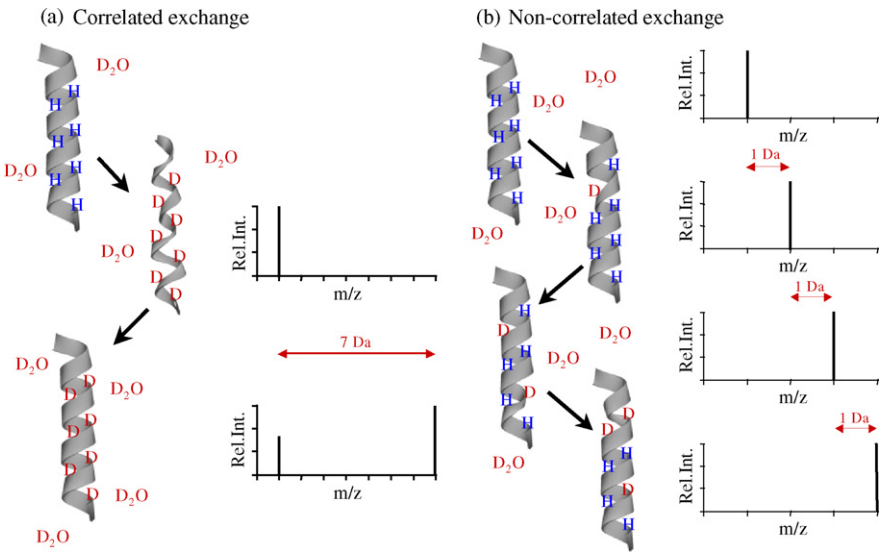

Fig. 6. Correlated vs. non-correlated exchange of amide hydrogens. This figure schematically illustrates the difference between correlated and non-correlated exchange for transient unfolding processes of an α-helix. Correlated exchange (left panel) occurs when the α-helix unfolds and all exposed amide hydrogens simultaneously undergo isotopic exchange before the α-helix refolds. This type of exchange is termed EX1, and the mass spectrometric signature for EX1 exchange is the appearance of a bimodal peak pattern (also depicted). Non-correlated exchange (EX2) occurs when local structural fluctuations expose a single amide hydrogen to the solvent whereby it undergoes exchange. Note that non-correlated exchange is also observed upon unfolding of larger chain segments when the refolding is fast compared to the intrinsic chemical exchange kinetics. Mass spectrometric analysis of EX2 type exchange yields a single peak that gradually increases in mass with exchange time (also depicted).

The cleaved variants of β_2m are much more prone to aggregate than β_2m wt [18]. We attribute the increased aggregation propensity of the cleaved ΔK58-β_2m variant to its increased unfolding rate as the unfolded state in general has been implicated as a key intermediate in the aggregation process for other proteins [42–44]. Interestingly, NMR and CE analyses have shown that ΔK58-β_2m is somewhat more prone to aggregate than cK58-β_2m [18]. For example, aggregation of ΔK58-β_2m was observed with one-dimensional ^{1}H NMR spectroscopy at 25 °C, but not for cK58-β_2m at this temperature. However, increasing the temperature to 37 °C also caused cK58-β_2m to aggregate. To investigate whether this difference reflects that the unfolding rate of ΔK58-β_2m is greater than that of cK58-β_2m, we have now determined the unfolding rate of cK58-β_2m in the temperature range 25–37 °C. Fig. 7 shows mass spectra obtained from a mixture of ΔK58-β_2m and cK58-β_2m after deuteration in PBS for various periods at 32 °C. In this experiment, the unfolding rate constants (k_u) for both cleaved variants can be measured simultaneously because the nondeuterated proteins differ by 128 Da in mass and are thus well separated in the mass spectra. Unfolding rate constants of 5.2×10^{-2} min^{-1} for ΔK58-β_2m and 3.3×10^{-2} min^{-1} for cK58-β_2m were determined at 32 °C by fitting the abundance of the low and high mass populations to a bi-exponential equation (Fig. 8). The corresponding half-lives are listed in Table 1. Interestingly, ΔK58-β_2m unfolds 1.6 times faster than cK58-β_2m at 32 °C. This finding prompted us to determine the temperature dependence of the unfolding rate constant for cK58-β_2m. Table 1 shows the half-lives for cK58-β_2m and ΔK58-β_2m at various temperatures. At temperatures below 37 °C ΔK58-β_2m unfolds faster than cK58-β_2m. Thus, at 25 °C the half-lives for unfolding are 116 and 161 min, respectively. These values reflect that the cleaved β_2m proteins have a very low kinetic stability compared to other globular protein. As an example, the half-life for unfolding of thioredoxin wt, which is a kinetically stable globular protein, is approximately 4 months at 25 °C [45]. Evolution appears to have ensured that most proteins have a high kinetic stability as unfolding in a crowded cellular environment may lead to the formation of toxic protein aggregates and eventually cell death. β_2m wt is of intermediate kinetic stability, i.e., it is more stable than the two cleaved forms (as shown in Fig. 5). Surprisingly, at 37 °C the unfolding rates of ΔK58-β_2m and cK58-β_2m are identical within experimental error. To further investigate this phenomenon, the activation energy for unfolding of cK58-β_2m, E_a, was obtained from the slope of an Arrhenius plot of the temperature dependence of the unfolding rate constant (Fig. 9). This plot yields a value of $E_a = 2.0 \times 10^2$ kJ/mol, which is ∼30 kJ/mol higher than the corresponding value for ΔK58-β_2m (1.7×10^2 kJ/mol) [17]. Thus, removal of Lys58 slightly decreases the barrier for unfolding. Using Arrhenius plots, the half-life for cK58-β_2m and ΔK58-β_2m at 35 °C was estimated to 12 and 10 min, respectively. The higher unfolding rate of ΔK58-β_2m relative to that of cK58-β_2m at temperatures below 37 °C correlates

Table 1
Half-lives for transient global unfolding of ΔK58-β_2m and cK58-β_2m in deuterated PBS at various temperatures

Temp. (°C)	$t_{1/2}$ (min)	
	cK58-β_2m	ΔK58-β_2m
37	8	8
32	21	13
27	105	63
25	161	116

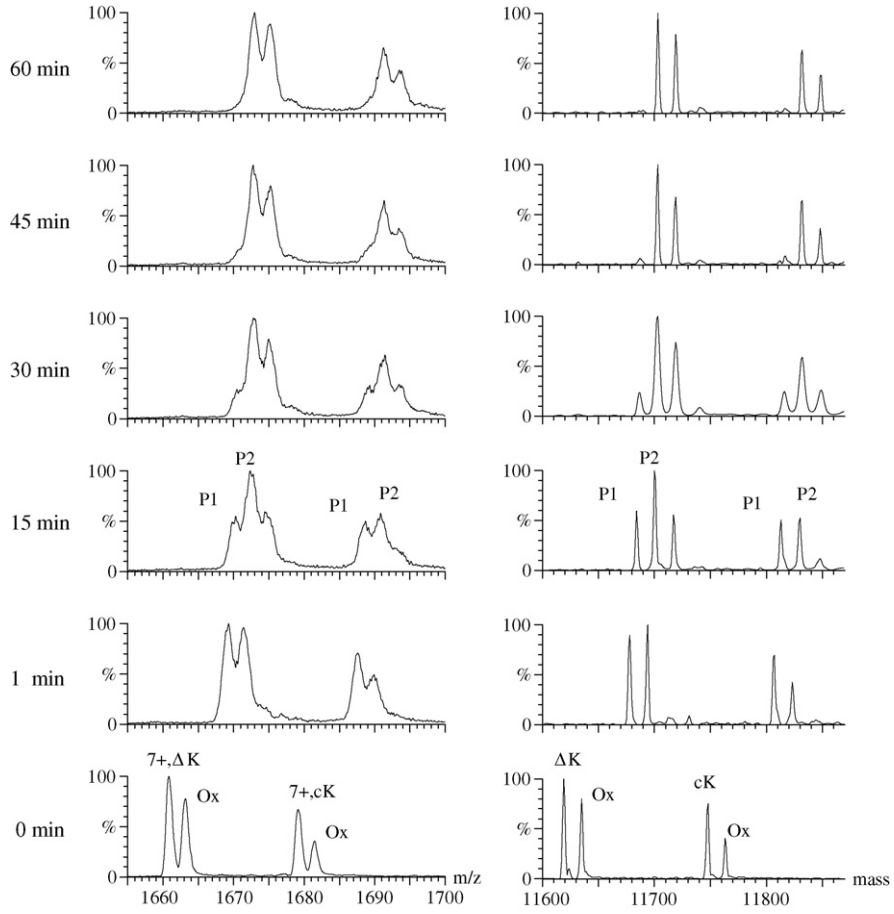

Fig. 7. Monitoring the transient global unfolding of ΔK58-β_2m and cK58-β_2m at 32 °C by amide $^1H/^2H$ exchange and mass spectrometry. Shown are electrospray ionization (ESI) mass spectra of a mixture of ΔK58-β_2m and cK58-β_2m obtained after various deuteration periods (given in minutes in the figure). In the left panel the region of the spectra with the $[M+7H]^{7+}$ charge state is displayed; Ox, Met99-oxidized species. Right panel shows the deconvoluted mass spectra. The spectra obtained at $t = 0$ min (i.e., lowest traces) show the nondeuterated proteins. See legend to Fig. 5 for explanation of P1 and P2.

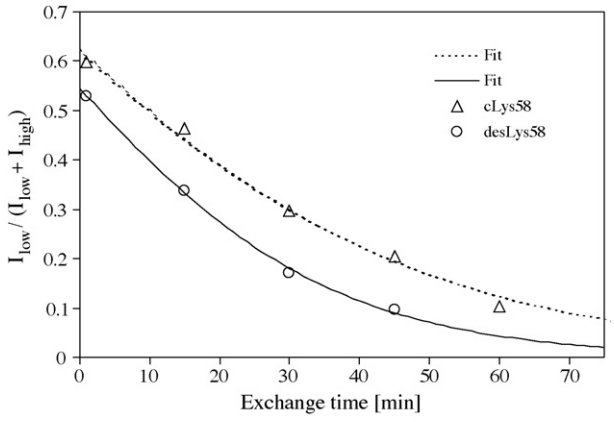

Fig. 8. Determination of rate constants for the transient global unfolding of ΔK58-β_2m and cK58-β_2m at 32 °C from the experiment shown in Fig. 7. Ratio of peak areas ($I_{low}/(I_{high} + I_{low})$) for ΔK58-$\beta_2$m (circles) and cK58-$\beta_2$m (triangles) were plotted as a function of exchange time. The lines show the fits to the experimental data using our previously described approach [17] and the constraint $k_u = k_{u,Ox}$. The fits yielded the unfolding rate constants, k_u, 5.2×10^{-2} min^{-1} and 3.3×10^{-2} min^{-1} for ΔK58-β_2m and cK58-β_2m, respectively.

with the increased propensity of ΔK58-β_2m to aggregate at 25 °C and 35 °C as measured by ^1H NMR spectroscopy and CE analyses, respectively [18]. It is important to note, however, that other factors may also be important for the difference in aggregation kinetics between the two cleaved variants. For example the unfolded state of ΔK58-β_2m may have different physicochemical properties that increases its ability to form aggregates [46].

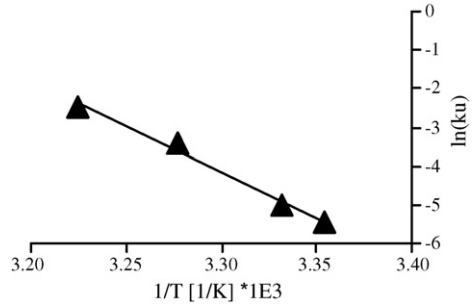

Fig. 9. Determination of activation energy for the transient global unfolding of cK58-β_2m. Arrhenius plot of $\ln(k_u)$ as a function of $1/T$ from which an activation energy, E_a, of 2.0×10^2 kJ/mol for unfolding was obtained from the slope ($-E_a/R$). The correlation coefficient, R^2, was 0.988.

4. Conclusions

CE rapidly provides information about the equilibrium distribution of conformers and allows for rapid screening of the effect of variations in physico-chemical parameters such as temperature, ionic strength, pH, metal ions, and protein concentration on conformer state and aggregation reactions. A more detailed qualitative and quantitative understanding of conformational dynamics, however, is particularly dependent on other techniques such as mass spectrometric monitoring of amide hydrogen ($^1H/^2H$) exchange rates as illustrated for β_2m in the present study. The combined results have allowed us to conclude that a similar global conformation and a similar unfolding process occur in both the intact and the lysine-58 cleaved forms of this molecule. The unfolding, however, occurs significantly faster in cleaved β_2m. The organic solvent-inducible alternative conformer which is electrophoretically indistinguishable from the variant conformer occurring under physiological conditions clearly corresponds to a much more open form of β_2m as evidenced by the isotopic exchange experiments.

The experiments together with previously reported results provide evidence that the formation of an unstructured species, resulting from a cooperative unfolding, is a critical event that is likely to trigger an aggregation process for β_2m. When the unfolding rate is accelerated the probability increases for a molecular encounter between two unfolded molecules. This process will lead to the formation of dimers and eventually higher order oligomers. Note that oligomeric species of wt-β_2m have recently been observed by noncovalent electrospray ionization mass spectrometry [47]. Our results strongly suggest that the first step in the molecular mechanism for fibril formation is a cooperative unfolding. The HX-MS experiments provide this information readily through analysis of the temporal evolution of mass changes in the analyte molecules. The HX-MS approach provides an analytical separation of species depending on their conformational experience, and is also more sensitive in the sense that it requires less material than NMR experiments where the signal from opened molecules is diluted and distorted by the reversibility of the reaction and the presence of unopened species. As a drawback, in the mass spectrometric experiments no information on the site of unfolding is readily available. However, localization within a few residues of the incorporated deuterons may be achieved by pepsin digestion of the labeled protein at conditions where the isotopic exchange is quenched. The resolution of this method will depend on the number and size of pepsin-generated peptides with overlapping sequences. Alternatively, gas phase fragmentation may lead to the desired site-specific information if hydrogen atom scrambling can be avoided [48,49]. This work is in progress and will further advance our understanding of pro-amyloidogenic unfolding reactions and aggregate formation and thus advance studies of ways to inhibit such events.

Acknowledgments

This paper is dedicated to Prof. Peter Roepstorff who has never failed to inspire us during the many years our two institutions have collaborated. T.J.D.J. would like to thank Peter for his wholehearted support and for great inspiration through all the years.

The studies reported herein have been supported by Lundbeckfonden, Apotekerfonden and Carlsbergfondet.

References

[1] L. Obici, V. Perfetti, G. Palladini, R. Moratti, G. Merlini, Biochim. Biophys. Acta 1753 (2005) 11.
[2] F. Gejyo, T. Yamada, S. Odani, Y. Nakagawa, M. Arakawa, T. Kunitomoto, H. Kataoka, M. Suzuki, Y. Hirasawa, T. Shirahama, Biochem. Biophys. Res. Commun. 129 (1985) 701.
[3] P.D. Gorevic, T.T. Casey, W.J. Stone, C.R. Diraimondo, F.C. Prelli, B. Frangione, J. Clin. Invest. 76 (1985) 2425.
[4] M. Jadoul, C. Garbar, H. Noel, J. Sennesael, R. Vanholder, P. Bernaert, G. Rorive, G. Hanique, d.S. van Ypersele, Kidney Int. 51 (1997) 1928.
[5] M. Okon, P. Bray, D. Vucelic, Biochemistry 31 (1992) 8906.
[6] J.M. Campistol, D. Bernard, G. Papastoitsis, M. Sole, J. Kasirsky, M. Skinner, Kidney Int. 50 (1996) 1262.
[7] R.P. Linke, J. Bommer, E. Ritz, R. Waldherr, M. Eulitz, Biochem. Biophys. Res. Commun. 136 (1986) 665.
[8] R.P. Linke, H. Hampl, S. Bartel-Schwarze, M. Eulitz, Biol. Chem. 368 (1987) 137.
[9] R.P. Linke, H. Hampl, H. Lobeck, E. Ritz, J. Bommer, R. Waldherr, M. Eulitz, Kidney Int. 36 (1989) 675.
[10] M.S. Stoppini, P. Arcidiaco, P. Mangione, S. Giorgetti, D. Brancaccio, V. Bellotti, Kidney Int. 57 (2000) 349.
[11] D.B. Corlin, J.W. Sen, S. Ladefoged, G. Lund, M.H. Nissen, N.H.H. Heegaard, Clin. Chem. 51 (2005) 1177.
[12] M.H. Nissen, O.J. Bjerrum, T. Plesner, M. Wilken, M. Rorth, Clin. Exp. Immunol. 67 (1987) 425.
[13] F. Chiti, E. De Lorenzi, S. Grossi, P. Mangione, S. Giorgetti, G. Caccialanza, C.M. Dobson, G. Merlini, G. Ramponi, V. Bellotti, J. Biol. Chem. 276 (2001) 46714.
[14] N.H.H. Heegaard, J.W. Sen, M.H. Nissen, J. Chromatogr. A 894 (2000) 319.
[15] N.H.H. Heegaard, P. Roepstorff, S.G. Melberg, M.H. Nissen, J. Biol. Chem. 277 (2002) 11184.
[16] N.H.H. Heegaard, J.W. Sen, N.C. Kaarsholm, M.H. Nissen, J. Biol. Chem. 276 (2001) 32657.
[17] N.H.H. Heegaard, T.J.D. Jørgensen, N. Rozlosnik, D.B. Corlin, J.S. Pedersen, A.G. Tempesta, P. Roepstorff, R. Bauer, M.H. Nissen, Biochemistry 44 (2005) 4397.
[18] M.C. Mimmi, T.J.D. Jørgensen, F. Pettirossi, A. Corazza, P. Viglino, G. Esposito, E. De Lorenzi, V. Bellotti, M. Pries, D.B. Corlin, M.H. Nissen, N.H.H. Heegaard, FEBS J. 273 (2006) 2461.
[19] A. Kameda, M. Hoshino, T. Higurashi, S. Takahashi, H. Naiki, Y. Goto, J. Mol. Biol. 348 (2005) 383.
[20] S.E. Radford, W.S. Gosal, G.W. Platt, Biochim. Biophys. Acta 1753 (2005) 51.
[21] S. Jones, J. Manning, N.M. Kad, S.E. Radford, J. Mol. Biol. 325 (2003) 249.
[22] F. Chiti, P. Mangione, A. Andreola, S. Giorgetti, M. Stefani, C.M. Dobson, V. Bellotti, N. Taddei, J. Mol. Biol. 307 (2001) 379.
[23] A.J. Borysik, S.E. Radford, A.E. Ashcroft, J. Biol. Chem. 279 (2004) 27069.
[24] M.I. Ivanova, M.J. Thompson, D. Eisenberg, Proc. Natl. Acad. Sci. U.S.A. 103 (2006) 4079.
[25] Y. Motomiya, Y. Ando, K. Haraoka, X. Sun, H. Morita, I. Amano, T. Uchimura, I. Maruyama, Kidney Int. 67 (2005) 314.
[26] H. Wadai, K. Yamaguchi, S. Takahashi, T. Kanno, T. Kawai, H. Naiki, Y. Goto, Biochemistry 44 (2005) 157.
[27] M. Monti, A. Amoresano, S. Giorgetti, V. Bellotti, P. Pucci, Biochim. Biophys. Acta 1753 (2005) 44.
[28] M.I. Ivanova, M.R. Sawaya, M. Gingery, A. Attinger, D. Eisenberg, Proc. Natl. Acad. Sci. U.S.A. 101 (2004) 10584.

[29] M.H. Nissen, B. Johansen, O.J. Bjerrum, J. Immunol. Methods 205 (1997) 29.
[30] W. Rist, M.P. Mayer, J.S. Andersen, P. Roepstorff, T.J.D. Jørgensen, Anal. Biochem. 342 (2005) 160.
[31] P.W. Atkins, Physical Chemistry, fifth ed., Oxford University Press, Oxford, 1994.
[32] N.H. Heegaard, T.J.D. Jørgensen, L. Cheng, C. Schou, M.H. Nissen, O. Trapp, Anal. Chem. 78 (2006) 3667.
[33] T.E. Wales, J.R. Engen, Mass Spectrom. Rev. 25 (2006) 158.
[34] J.S. Milne, L. Mayne, H. Roder, A.J. Wand, S.W. Englander, Protein Sci. 7 (1998) 739.
[35] N.H.H. Heegaard, L. Rovatti, M.H. Nissen, M. Hamdan, J. Chromatogr. A 1004 (2003) 51.
[36] J. Lim, R.W. Vachet, Anal. Chem. 76 (2004) 3498.
[37] A. Hvidt, S.O. Nielsen, Adv. Protein Chem. 21 (1966) 287.
[38] S.W. Englander, L. Mayne, Y. Bai, T.R. Sosnick, Protein Sci. 6 (1997) 1101.
[39] C.B. Arrington, L.M. Teesch, A.D. Robertson, J. Mol. Biol. 285 (1999) 1265.
[40] A. Miranker, C.V. Robinson, S.E. Radford, R.T. Aplin, C.M. Dobson, Science 262 (1993) 896.
[41] H. Maity, W.K. Lim, J.N. Rumbley, S.W. Englander, Protein Sci. 12 (2003) 153.
[42] D.R. Booth, M. Sunde, V. Bellotti, C.V. Robinson, W.L. Hutchinson, P.E. Fraser, P.N. Hawkins, C.M. Dobson, S.E. Radford, C.C.F. Blake, M.B. Pepys, Nature 385 (1997) 787.
[43] M. Dumoulin, A.M. Last, A. Desmyter, K. Decanniere, D. Canet, G. Larsson, A. Spencer, D.B. Archer, J. Sasse, S. Muyldermans, L. Wyns, C. Redfield, A. Matagne, C.V. Robinson, C.M. Dobson, Nature 424 (2003) 783.
[44] F. Chiti, C.M. Dobson, Annu. Rev. Biochem. 75 (2006) 333.
[45] R. Godoy-Ruiz, F. Ariza, D. Rodriguez-Larrea, R. Perez-Jimenez, B. Ibarra-Molero, J.M. Sanchez-Ruiz, J. Mol. Biol. 362 (2006) 966.
[46] F. Chiti, M. Stefani, N. Taddei, G. Ramponi, C.M. Dobson, Nature 424 (2003) 805.
[47] A.M. Smith, T.R. Jahn, A.E. Ashcroft, S.E. Radford, J. Mol. Biol. 364 (2006) 9.
[48] T.J.D. Jørgensen, H. Gårdsvoll, M. Ploug, P. Roepstorff, J. Am. Chem. Soc. 127 (2005) 2785.
[49] T.J.D. Jørgensen, N. Bache, P. Roepstorff, H. Gårdsvoll, M. Ploug, Mol. Cell. Proteomics 4 (2005) 1910.
[50] C.H. Trinh, D.P. Smith, A.P. Kalverda, S.E. Phillips, S.E. Radford, Proc. Natl. Acad. Sci. U.S.A. 99 (2002) 9771.